Hindawi
Adsorption Science & Technology
Volume 2022, Article ID 3669652, 16 pages
https://doi.org/10.1155/2022/3669652

Research Article

Removal of Toxic Metal Ions from Aqueous Solutions in Integrated Clay Adsorption and Electroflotation

Raimundo Nonato Pereira Teixeira,[1] Vicente Oliveira Sousa Neto,[2] Juliene Tomé Oliveira,[3] Lucas Fontenele Amorim,[3] Eliezer Fares Abdala Neto,[3] Diego de Quadros Melo,[4] Henrique Douglas Melo Coutinho,[1] Bonglee Kim,[5] Jorge Marcell Coelho Menezes,[1] and Ronaldo Ferreira do Nascimento[3]

[1]*Department of Biological Chemistry, Laboratory of Research in Natural Products, Regional University of Cariri (URCA), 63100-000 Crato, CE, Brazil*
[2]*State University of Ceara, Center of Education, Sciences and Technology of Region of Inhamuns-CECITEC, BR 116, s/n, Bairro Bezerra e Souza, Tauá, Ceará, Brazil*
[3]*Department of Analytical Chemistry and Physico-Chemistry, Federal University of Ceará, Rua do Contorno, S/N, Campus do Pici, Bl. 940 CEP:, 60451-970 Fortaleza, CE, Brazil*
[4]*Department of Physical, Federal University of Ceará, Fortaleza, Ceara 60455-900, Brazil*
[5]*Department of Pathology, College of Korean Medicine, Kyung Hee University, Seoul 02447, BK, Republic of Korea*

Correspondence should be addressed to Henrique Douglas Melo Coutinho; hdmcoutinho@gmail.com and Bonglee Kim; bongleekim@khu.ac.kr

Received 20 February 2022; Revised 16 May 2022; Accepted 2 July 2022; Published 20 July 2022

Academic Editor: Randa Khalifa

Copyright © 2022 Raimundo Nonato Pereira Teixeira et al. This is an open access article distributed under the Creative Commons Attribution License, which permits unrestricted use, distribution, and reproduction in any medium, provided the original work is properly cited.

Most galvanic process industries treat their effluents by chemical precipitation methods. Such a method produces an amount of galvanic sludge that is often disposed of inappropriately to the environment, causing major environmental damage. These rejects present high concentrations of toxic metallic ions, such as copper (Cu(II)), lead (Pb(II)), nickel (Ni(II)), and cadmium (Cd(II)). Several alternatives have been proposed to contribute in a cheaper and efficient way to treat these effluents. This study aimed to describe the results obtained in the removal of the concentrations of Cu(II), Ni(II), Cd(II), and Pb(II) ions, present in an aqueous solution, by the use of a hybrid system combining the adsorption and electroflotation processes simultaneously. The adsorbent materials used were two Brazilian soil clays classified as sodium clay (SC) and ferric clay (FC). For the electroflotation process, aluminum, iron, and stainless-steel electrodes were used. The obtained data showed good efficiency in the removal of the four metallic ion concentrations. The best results presented a reduction in the concentration of Cu(II), Ni(II), Cd(II), and Pb(II) ions of 50.11%, 36.71%, 21.59%, and 23.43%, respectively, when it was used the hybrid system formed by the ferrous clay as adsorbent and the aluminum electrode for the electroflotation process.

1. Introduction

Highly acidic heavy metal laden effluents, originating from electroplating industry, are of major concern and increasingly subjected to stringent regulations in the way that they must be treated prior to their discharge into the environment. In electroplating units, water is used for various processes, thus eventually forming electroplating wastewaters (EWW), which are highly enriched in acid contents and heavy metals (Zn, Fe, Cr, Ni, Cd, Au, and Cu), which render them severely corrosive and polluting in nature. According to Nagajyoti et al. [1], the accumulation of heavy metals in soils causes concern for agricultural production, because it has adverse effects on commercialization and food safety and its phytotoxicity affects the growth of the crop and also on the environmental health of soil organisms.

Their adverse effect on the environment can be neutralized by the application of purification methods. Various techniques have been employed so far, including adsorption, physicochemical treatment, membrane filtration, ion exchange, and electrochemical treatment [2].

Electrochemical methods have been shown so far as a good alternative to the traditional physicochemical methods in water treatment [3]. In this context, electroflotation-coagulation has played an important role among the techniques for the treatment of industrial wastewater. And this is due to its versatility, in an operational mode as the efficiency of contaminant removal. Electroflotation-coagulation is a process based on the electrodissolution of the metal ions of anodes by electrolytic oxidation. Aluminum and iron metals have been commonly used as electrodes as they are cheap and easily available. The reactions occurring in an electrochemical cell for an aluminum electrode are shown below.

At the cathode:

$$2H_2O + 2e^- \longrightarrow H_2\,(g) + 2OH^-, \quad (1)$$

At the anode:

$$Al(s) \longrightarrow Al^{+3}(aq) + 3e^-, \quad (2)$$

In the solution:

$$Al^{+3}\,(aq) + 3H_2O \longrightarrow Al(OH)_3(s) + 3H^+(aq). \quad (3)$$

The aluminum hydroxide flakes act as adsorbents for toxic metal ions. Furthermore, the toxic metal ions combine with the electrogenerated OH^- ions at the cathode and precipitate in the form of their insoluble hydroxides. Both phenomena act synergistically leading to a rapid removal of toxic metal pollutants from the aqueous solution [4].

According to Gupta, Nayak, and Agarwal [5] and Saleh and Gupta [6], the adsorption has been developed as an efficient method for the removal of toxic metals from contaminated water and soil. A variety of adsorbents have been used for the removal of metal ions, such as clays [7–10], zeolites [11, 12], dried plant parts [13, 14], and activated carbon [15, 16].

The reactors used to removal of pollutants by electroflotation are small and compact and present low maintenance and operation costs when compared to other flotation processes.

Some works have proposed systems using two or more processes for removing toxic metal ions from aqueous solutions [17]. Among these hybrid processes are included microfiltration-electrocoagulation [18] adsorption-microfiltration processes [19], and adsorption-ion exchange [20].

The hybrid system that combines adsorption and electrocoagulation has been shown to be effective for the removal of organic and inorganic pollutants. Many studies report on the treatment of effluents contaminated by organic pollutants using this hybrid system. Pekka et al. (2018) [21] tested the efficiency of this system in removing total carbon from an electrocoagulation system accompanied by adsorption with activated carbon. However, some researchers have tried to investigate the hybrid system in the removal of inorganic pollutants, and some studies report on the use of the two techniques combined in the treatment of effluents contaminated by metals. Sohail et al. (2020) [22] showed that the hybrid system was efficient for the removal of Cr, Cu, and Zn, obtaining a maximum removal capacity of 97.44% for Cr, 97.45% for Cu, and 74.18% for Zn. Elbert et al. (2020) [23] tested the efficiency of this hybrid system that showed a calcium removal capacity of 88% ($6.0\,mg.L^{-1}$) and 72% of strontium ($0.4\,mg.L^{-1}$).

The results found that a combined hybrid system is very promising. Thereby, the objective of this paper is to investigate the use of a hybrid system which associates the process of adsorption onto clays with electroflotation-coagulation for removal of Cu(II), Ni(II), Cd(II), and Pb(II) in aqueous systems.

2. Materials and Methods

2.1. Adsorbents. The clays samples used in this study were given from the Bentonisa Company in Campina Grande, Paraíba, Brazil. The sodium and ferric clays were used in their raw form, without any prior treatment. The clays were sieved, and the material was separated in a range of 0.074-0.105 mm.

2.2. Characterization Methods. X-ray diffraction (XRD) patterns were recorded at a Philips X'Pert X-ray diffractometer, with a CuKa radiation for crystalline phase with a routine power of 1600 W (40 kV and 40 mA). A wavelength dispersive X-ray fluorescence spectrometer (model ZMS Mini II, Rigaku) was used to obtain the X-ray fluorescence spectra. The surface area analysis was determined by isotherms of adsorption/desorption of N_2 (isotherms Brunauer, Emmett and Taller - BET) and held in a porosimeter (brand: Quantachrome, Model: NOVA 1200), and the data was exported using the Autosorb software. Sample preparation was performed for 12 hours under vacuum at 110 °C. The pore size distribution (PSD) was determined using the BJH method, which is a method to determine pore size distribution of a mesoporous solid based on the Kelvin equation and provides a much more informative result for a pore size distribution. These exchange capacities (EC) were conventionally expressed in meq/100 g [24], which is numerically equal to centimoles of charge per kilogram of exchanger (cmol(+)/kg). These values were estimated using the ammonium acetate method. The soil sample is extracted with a 1 M NH_4OAc solution at pH = 7.00. The soil-solution slurry is shaken for 2 h, and the solution is separated from the solid by centrifugation The addition of NH_4^+ in excess to the soil displaces the rapid exchangeable alkali and alkaline cations from the exchange sites of the soil particles [25].

2.3. Batch Adsorption Experiments. Analytical-grade chemicals and ultrapure water (Millipore Direct Q3 Water Purification System) were used to prepare the solutions.

Monoelement and multielement stock solutions of Ni(II), Cu(II), Cd(II), and Pb(II) (500 mg·L^{-1}) were prepared with $Ni(NO_3)_2{\cdot}6H_2O$, $Cu(NO_3)_2{\cdot}3H_2O$ $Cd(NO_3)_2{\cdot}4H_2O$, and $Pb(NO_3)_2$ (Merck, São Paulo, Brazil), respectively. The acetate buffer solution pH 5.5 was prepared with sodium acetate and glacial acetic acid. NaOH (0.10 mol·L^{-1}) and HCl (0.10 mol·L^{-1}) solutions were used for pH adjustments. Erlenmeyers (50.0 mL) and an orbital shaker device (Marconi, Brazil) operating at 150 rpm and 28 ± 2°C were used in the experiments. The adsorbents (50.0 mg) and the respective solutions (25.0 mL) containing the analytes were added to each flask. Equilibrium concentrations of the toxic metals were determined by using an atomic absorption spectrophotometer (VARIAN model AA240FS) with an air acetylene flame.

The equilibrium adsorption capacity of the adsorbent is calculated as follows:

$$q_e = \frac{\left(C_0 - C_{eq}\right)}{w} * V, \tag{4}$$

where q (mg g^{-1}) is the metal uptake of metal ion, C_o is the initial concentration, C_{eq} is the equilibrium concentration, V is the volume in L, and w is the mass of adsorbent in grams.

2.4. Adsorption Isotherms. To study adsorption isotherm, an orbital shaker table was used at a speed kept at 150 rpm. An adsorbent mass (50 mg) was mixed with solutions (25.0 mL) of each metal ion solution, at concentrations ranging from 40 to 300 (mg.L^{-1}). All experiments were performed in triplicate. The optimum pH used was 5.5 acetate-acid acetic buffer with an equilibration time of 1 h at 28 ± 2° C. At the end of the adsorption process, the supernatant was filtered, and the residual metal ion concentrations were determined by atomic absorption spectrophotometer (AAS). The amounts of adsorbed metals (mg g^{-1}) were determined from the concentrations before and after the equilibration time using Equation (4).

For an evaluation of the adsorption isotherms, the following statistical tools were used: R^2 (Equation (5))), $Radj^2$ (Equation (6))), SSE (Equation (7)), Hybrid (Equation (8)), and %Error (Equation (9)), where z: number of experimental points; q_{exp}: experimental adsorption capacity (mg g^{-1}); q_{exp} *: average of experimental adsorption capacity values (mg g-1); q_{calc}: calculated adsorption capacity (mg g^{-1}); and q_{max_exp}: maximum experimental adsorption capacity (mg g^{-1}).

To be considered adequate, the model must present the highest values of R^2 and $Radj^2$ and the lowest values of SSE, Hybrid, and %Error [26, 27]:

$$R^2 = \frac{\sum_i^z \left(q_{calc} - q_{\exp} *\right)2}{\sum_i^z \left(q_{calc} - q_{\exp *}\right)2 + \sum_i^z \left(q_{calc} - q_{\exp}\right)^{Ç}}, \tag{5}$$

$$R^2_{adj} = 1 - \frac{z-1}{z-(k-1)}\left(1 - R^2\right), \tag{6}$$

$$SSE = \sum_{i=1}^{z} \left(q_{\exp} - q_{calc}\right)^{Ç}, \tag{7}$$

$$Hybrid = \frac{100}{z-k}\sum_{i=1}^{z}\left(\frac{\left(q_{\exp} - q_{calc}\right)^{Ç}}{q_{\exp}}\right), \tag{8}$$

$$\%Error = \left|\frac{q_{max\_exp} - q_{max}}{q_{max}}\right|100, \tag{9}$$

2.5. Adsorption Kinetics. Adsorption kinetics studies allow the evaluation of the extent of adsorbate removal, as well as the identification of the predominant mechanisms involved in the adsorption process. For this, a multielement solution (100.0 mg·L^{-1}) was continuously shaken (150 rpm) at pH 5.5. The metal ion equilibrium concentrations were analyzed for adequate time interval (2, 4, 6, 8 10, 15, 20, 30, 40, and 60 min). Adsorption capacities were calculated, using the Equation (4), for each studied time.

2.6. Adsorption Electroflotation-Coagulation Experiments. In the studies with the hybrid system adsorption (electroflotation-coagulation), a series of tests were initially performed with the clays (3 g) associated with the hybrid system of electroflotation-coagulation using multielement solution (300 mg L^{-1}) with four ions (Ni(II), Cu(II), Cd(II), and Pb(II)) at pH 5.5. The operating conditions of the apparatus used in the testing of hybrid systems with adsorption (electroflotation-coagulation) are shown in Figure 1.

The electroflotation-coagulation process was performed on conditions as follows: 500.0 mL of synthetic effluent into 1000 mL cubic reactor. The electroreduction conditions were carried out with stainless steel, iron, and aluminum electrode plates (total area for a set of electrodes 50 cm^2 (10 × 5 cm), amount of electrodes per compartment of 2 units, and distance between plates of 1.5 mm. Voltage and electrical current were measured by supplies (Hayama® HY-125™, 220-12 V/5A, and total power 200 W) for an average current applied to a set of electrodes of 0.9 A, current density of 18 mA cm^{-2}, and consumption of 0.02 KWh L^{-1} for 20 minutes. The treatment procedure was run in duplicate. To evaluate the removal capacity for each hybrid system, we used the equation proposed for Grigorov and Alexandrova [28]:

$$\%Removal = \left(1 - \frac{C_f}{C_i}\right)x100, \tag{10}$$

where C_f is the final concentration and C_i is the initial concentration of the metal ion present in the solution.

2.6.1. Effect of Time of Operation and Initial Concentration in Removal of Toxic Metal Ion Monoelement System. The experiments were done using monoelementary solutions with concentrations of approximately 300 mg L^{-1} for times

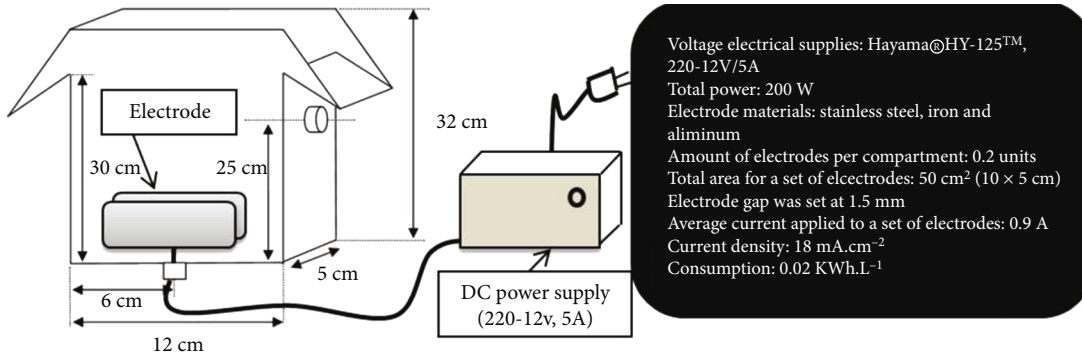

Figure 1: Electroflotation-coagulation reactor in laboratory scale used in the experiments and WRD patterns of the samples.

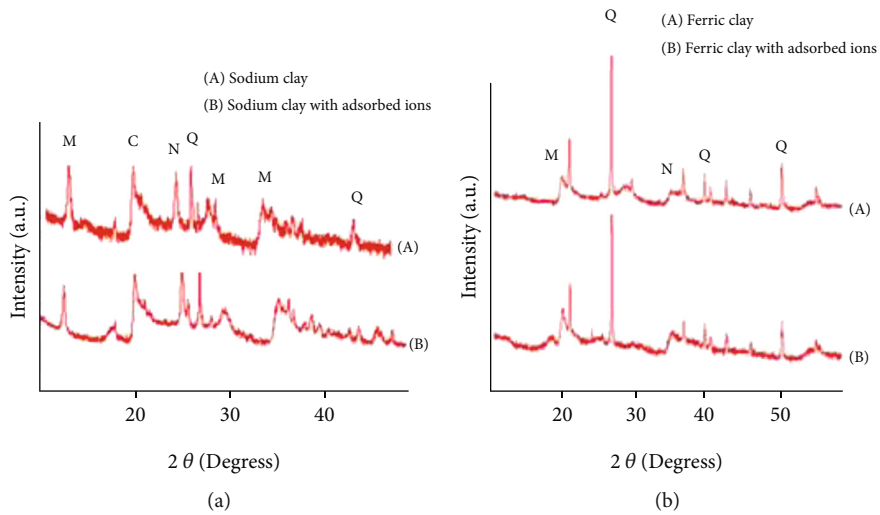

Figure 2: X-ray diffractogram of the clays before (a) and after (b) the four metal ions adsorption. 2 (a) Sodium clay and 2 (b) ferric clay. Ckaolinite ($Al_2H_4O_9Si_2$), M montmorillonite (Na, Ca), (Al,Mg) $2Si_4O_{10}$ $(OH)_2.xH_2O$), N-nontronite ($Fe_2H_{10}Na_{0,30}O_{16}Si_4$), Q-quartz ($SiO_2$).

of 2, 4, 6, 8, and 10 minutes. According to Sahu [29], many studies evaluate the influence of the initial concentration. To evaluate the effect of the initial concentration of metal ions, three different concentrations were prepared with the values 100, 250, and 500 mg L^{-1}.

2.6.2. Removal of Toxic Metal Ion Multielement Systems. The concentration of toxic metal ions ranges from 40 to 500 mg L^{-1}. Initially, tests using only the electrodes were performed without the addition of clays to evaluate the effect of the techniques separately, and experiments were then done with the hybrid system adsorption electrocoagulation-coagulation.

3. Results and Discussion

3.1. Clay Sample Characterizations

3.1.1. X-Ray Diffractograms. The X-ray diffractograms of sodium and ferric clays, before and after the adsorption of the four metallic ions, are shown in Figures 2(a) and 2(b), respectively. Characteristics of an amorphous material with broad peaks can be observed. This follows from the fact that the clay minerals have not undergone any previous treatment and the analysis was done with the sample in the raw state. Nevertheless, one can check some typical patterns of bentonite, with the presence of clay minerals from the group of montmorillonites with interplanar distance (d001) in 14.053 Å [30], as well the presence of quartz with interplanar distance (D101) at 3.34 Å [31] and kaolinite (D002) 3.59 Å [32]. It is observed by the XRD pattern (Figure 2(a)) that there were no changes in the clay mineral structure after adsorption of the four ions. This is to be expected since the chemical species present in the clay mineral (such as quartz, kaolinite, and montmorillonite) do not suffer any transformation with the presence of these four new ions. The structures of clay minerals are usually affected by processes such as calcination, acid, alkaline attack, or pillarization [33].

XRD of the ferric clay, before and after the adsorption of the four ions (Figure 2(b)), present the existence of characteristic peaks of quartz (D100) with a basal spacing of 4.26 Å [29], in montmorillonite 13.60 Å [30], and nontronite at 13.30 Å [34]. There were also no changes in the structures of clay after adsorption of the four metal ions as shown in curve B.

Table 1: Chemical composition (% by weight) obtained for X-ray fluorescence..

Clay	%Si	%Al	%Ca	%Fe	% K	%Zn	%Cu	%Ni	%Cd	%Pb	%Mn	%Ti
SC	56.64	20.96	9.805	6.332	5.971	0.287	—	—	—	—	—	—
SC/ADS	41.35	14.66	4.876	5.076	4.072	0.174	0.824	2.051	1.869	23.72	0.440	0.776
FC	59.16	6.377	5.931	25.27	0.740	—	—	—	—	—	0.184	1.819
FC/ADS	38.09	10.06	2.125	21.63	0.732	—	10.99	6.512	1.323	6.764	—	1.527

CS: sodium clay; CS/ADS: sodium clay with adsorbed ions; CF: ferric clay; CF/ADS: ferric clay with adsorbed ions.

3.1.2. X-Ray Fluorescence. Table 1 presents the results obtained by the X-ray fluorescence for two clays before and after the metal ion adsorption. It can be seen that the two clays before the adsorption process are predominantly of Si and Al elements in the form of oxides. Sodium clay has a higher content of Al_2O_3 than ferric clay. The amount of SiO_2 is due to silicates such as feldspars and micas. Titanium and manganese oxides appear in small amount in the ferric clay, but they were not detected in sodium clay. The occurrence of calcium in the two types of clays can be due to cation exchange, since the difratograms of these clays do not show the presence of calcite, dolomite, or gypsum. On other hand, the presence of K in clays is almost entirely due to feldspar or exchangeable cations.

In general, the chemical composition of the clays tends to vary due to two main factors such as the different smectite and isomorphic substitutions in the presence of associated impurities. The results presented in Table 2 confirm the incorporation of the four metal ions in both clays after the adsorption process. Sodium clay showed that the highest amount of Pb(II) retained (23.72%). This is due to the fact that clay contains (in its chemical composition) the montmorillonite mineral, which has more negative adsorption sites found that of other clay minerals. In clay, ferric ion which had a higher amount retained is Cu(II), about 10.99%.

The average size of the clay particles was about 8.8×10^{-3} cm. The surface area of sodium clay was 8.48 and for the ferric clay 59.2 $m^2\,g^{-1}$, by means of BET method using nitrogen. The exchange capacities (EC) were 13.6 meq/100 g to sodium clay and 11.9 meq/100 g to ferric clay.

3.1.3. BET and EC. Figure 3 presents the BET surface area and pore size distribution. The values of the specific surface areas of the clays samples were 8.478 and 59.2 $m^2.g^{-1}$ for sodium and ferric clays, respectively. It was observed that the ferric clay presented a specific area about seven times larger than the sodium clay. A total pore volume of 9.858×10^{-2} $cm^3.g^{-1}$ was observed for the sodium clay and 1.009×10^{-1} $cm^3.g^{-1}$ for the ferric clay, respectively.

It is noted that the curves presented for any two clays exhibit hysteresis and are similar to type IV isotherm, characterized by the presence of mesopores, with pores of intermediate diameters of between 20 and 500 Å [35], in which formation multilayer adsorption is possible, but with limited size of the porosity of the material. The predominance of mesopores with average diameters of 42.32 Å was observed in sodium clay and 48.25 Å in ferric clay. The exchange capacities (EC) were 13.6 meq/100 g in sodium clay and 11.9 meq/100 g in ferric clay.

3.2. Batch Adsorption

3.2.1. Adsorption Isotherm Models. The Langmuir adsorption model [36] has been successfully used to explain the metal's adsorption from aqueous solutions and is based that the maximum adsorption corresponds to a saturated monolayer of solute molecules on the adsorbent surface with no lateral interaction between the adsorbed metal ions. The Freundlich isotherm [37] is an empirical equation employed to describe heterogeneous systems.

Temkin and Pyzhev [38] considered the effects of some indirect sorbate/adsorbate interactions on adsorption isotherms and suggested that because of these interactions, the heat of adsorption of all the molecules in the layer would decrease linearly with coverage.

Comparing the experimental results and the parameters obtained by the models used, it was realized that they were similar to other results obtained by other researchers. Rybicka et al. [39] studied the adsorption capacity of Cu(II), Pb(II), Ni(II), Cd(II), and Zn(II) in three clays and observed that montmorillonite adsorbs the following descending order Pb > Cd ~ Cu > Zn. Potgieter et al. [40] studied the adsorption capacity of Pb(II), Ni(II), Cr(II), and Cu(II) by the paligorsquita adsorbent and obtained the following descending order for adsorption capacity Pb > Cr > Ni > Cu.

Figure 4 presents the experimental curves in comparison with the applied models.

Table 3 shows the results obtained in this study compared with other obtained by the literature.

3.2.2. Sorption Kinetics. The following kinetic models were studied in this work: pseudo-second order proposed by Ho and Mckay [41] and Elovich equation [42].

Analyzing the data presented in Tables 4 and 5, it is possible to observe that the pseudo-second-order model presented a better approximation of the experimental value (R^2), compared to the Elovich model.

Table 2: Langmuir, Freundlich, and Temkin isotherm models' constants and coefficients of determination for adsorption of Cu(II), Ni(II), Cd(III), and Pb(III) onto sodium clay (SC) and ferric clay (FC).

Íons	Clay	Langmuir model							Freundlich model			Temkin model		
		Qmax ± SD	K_L	R^2	%Error	R^2_{adj}	SSE	*Hybrid*	*N*	K_F	R^2	B	K_T	R^2
Cu(II)	SC	35.71 ± 1.2	0.065	0.994	12.5	0.974	12.4	6.8	6.261	15.39	0.979	7.613	0.515	0.842
	FC	34.72 ± 1.2	0.036	0.986	5.4	0.956	9.5	4.3	3.098	5.583	0.988	6.076	0.690	0.977
Ni(II)	SC	26.84 ± 0.7	0.035	0.990	4.7	0.972	13.8	6.9	2.785	3.705	0.959	4.917	0.582	0.961
	FC	15.94 ± 0.4	0.198	0.986	4.1	0.961	14.4	7,5	8.682	8.654	0.622	1.366	523.8	0.591
Cd(II)	SC	26.81 ± 0.6	0.044	0.983	5.4	0.957	15.5	8.7	2.840	2.815	0.887	5.593	0.283	0.949
	FC	10.93 ± 0.4	0.259	0.989	8.9	0.954	18.4	8,9	7.716	5.476	0.787	1.189	47.09	0.740
Pb(II)	SC	50.76 ± 1.8	0.017	0.978	9.1	0.969	21.9	9.7	1.862	2.531	0.928	10.26	0.211	0.967
	FC	11.61 ± 0.3	0.093	0.995	4.2	0.975	7.4	3.8	4.249	3.358	0.828	1.891	2.133	0.841

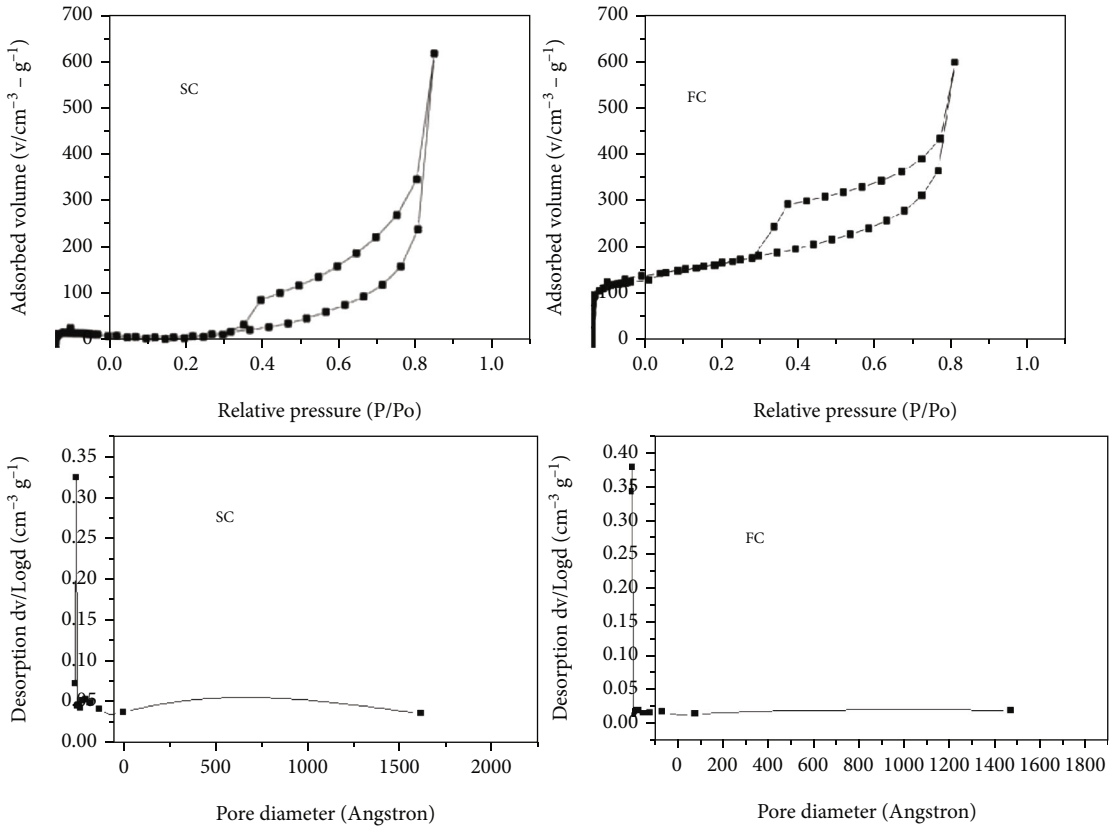

Figure 3: BET surface area plots and pore size distribution of the sodium clay (SC) and ferric clay (FC).

The fact that the second-order kinetics is the best fit model for the adsorption of metal ion onto clay indicates that the adsorption rate of all metal ion depends on the concentration of ions at the adsorbent surface and the behavior over a whole range of adsorption is in agreement with chemical adsorption being the rate controlling step [43, 44].

The K_2 results indicate that the adsorption of the four ions is favorable in both clays. The values only confirm this because the values were low in all systems studied.

3.2.3. Diffusion Models. The mechanisms and rate controlling steps that affect the kinetics of adsorption can be determined by fitting the kinetic experimental results to the Weber's intra-particle diffusion [45] and Boyd et al.'s [46] models.

Figures 5–12 present the experimental and theoretical curves for Cu(II), Ni(II), Cd(II), and Pb(II) ions from sodium and ferric clays.

These results can be explained because the clays have a very great swelling capacity by the incorporation of water

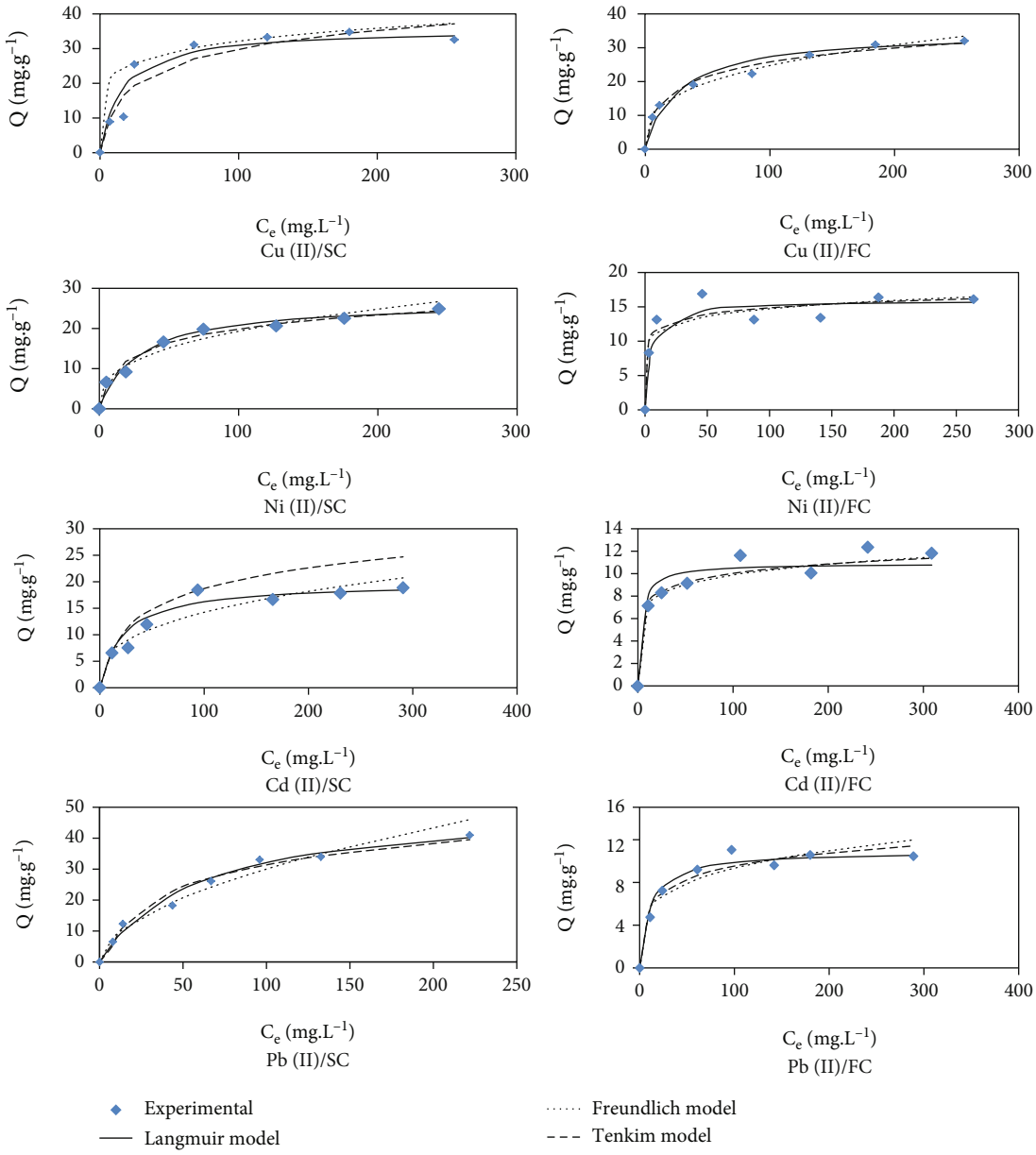

Figure 4: Experimental results of the adsorption equilibrium of Cu(II), Ni(II), Cd(II), and Pb(II) in SC and FC clays and theoretical curves from Langmuir, Freundlich, and Tenkim models at pH 5.5, T = 28°C, and stirring speed of 150 rpm.

in its structure. The clays which have interlayer cations present the properties well in the presence of water, increasing to several times its initial volume; this is because interlayer cations allow multiple water molecules and are adsorbed by increasing the distance between the layers and thus separating the clay particles from each other [47]. According to Glendening and Feller [48], the chemical mechanism of hydration of interlayer cations for these types of clay minerals is mainly through electrostatic interactions that maximize charge-dipole attraction and minimize water-water repulsion.

3.3. Hybrid System Adsorption Electroflotation-Coagulation. Initially, tests were conducted to discover the best operating conditions for hybrid systems. In order to do this, three types of electrodes were tested. The electrodes which were tested were as follows: an aluminum electrode, a stainless-steel electrode, and an iron electrode. The percentage of removal of ions in solution was calculated. The results for the removal percentages are presented in Table 6.

In Table 6, it is possible observe that the stainless-steel electrode combination with clays showed a lower removal capacity compared with the other two systems evaluated. The results of four systems were evaluated: (aluminum electrode/sodium clay), (iron electrode/sodium clay), (iron electrode/ferric clay), and (iron electrode/ferric clay). The assessments made with these systems note the operation time and the effect of the initial concentration.

To evaluate the contact time in the adsorption test, aliquots were removed at two-minute intervals, and the

Table 3: Comparison of Langmuir parameters on the adsorption of the ions Cu(II), Ni(II), Cd(II), and Pb(II) in these work clays and the literature.

Metal ion	Adsorbent	Qmax (mg/g)	KL (L/mg)	Reference
Cu(II)	Natural montmorillonite	31.8	192.8	Gupta and Bhattacharyya, (2011)
	Clays containing montmorillonite	30.9	0.0147	Oubagaranadin and Murthy, (2010)
	Sodium clay	35.71	0.065	This study
	Ferric clay	34.72	0.036	This study
Ni(II)	Calcined montmorillonite	21.14	137.54	Bhattacharyya and Gupta (2006)
	Paligorsquita with acid activation	93.02	0.0016	Chen and Wang (2007)
	Sodium clay	26.84	0.035	This study
	Ferric clay	15.948	0.198	This study
Cd(II)	Turkish illitic clay	13.09	0.0065	Ozdes et al., (2011)
	Ca-montmorillonite modified with humic acid	14.14	0.030	Wu et al. (2011)
	Sodium clay	26.81	0.044	This study
	Ferric clay	10.93	0.259	This study
Pb(II)	Clay mixture containing boron	79.4	0.11	Olgun and Atar (2012)
	Turkish illitic clay	53.76	0.069	Ozdes et al. (2011)
	Sodium clay	50.76	0.017	This study
	Ferric clay	11.614	0.093	This study

Table 4: Parameters of kinetic models for adsorption of Cu(II), Ni(II), Cd(II), and Pb(II) in clays: sodium (SC) and ferric (FC). Experimental conditions: acetate buffer pH = 5.5, T = 28°C. Initial concentration of ions = 100 mg L^{-1}.

Ion	Clay	Ho model				Elovich model			
		Qexp	Qcal	K2	R2	Qcal	α	β	R2
Cu(II)	SC	27.93	28.16	0.084	0.999	28.38	3.97×1027	2.37	0.722
	FC	21.24	21.50	0.195	0.999	22.12	4.42×1020	2.39	0.670
Ni(II)	SC	20.90	20.70	0.044	0.993	20.40	2.4×105	0.818	0.713
	FC	17.29	17.12	0.270	0.999	17.71	1.6×106	1.035	0.782
Cd(II)	SC	16.41	16.66	0.065	0.999	16.86	2.3×103	0.720	0.898
	FC	18.82	18.83	0.184	0.999	19.35	2.5×107	1.087	0.515
Pb(II)	SC	33.87	33.55	0.056	0.999	34.66	1.4×103	0.357	0.931
	FC	32.80	33.11	0.760	0.999	43.74	1.3×106	0.539	0.537

Q_{cal} (mg g^{-1}); K_2 (g mg^{-1} min^{-1}); α (mg g^{-1} min^{-1}); and β (mg g^{-1}).

amounts of the remaining metal ions in solutions were determined.

In all the systems studied, it was verified that very long times were not required for the system to remove the maximum amount of metal ions. This result is important, since the power consumed is one of the factors that must be taken into consideration to assess the operation of the system. Another fact that can be noted is that longer the system running the greater, amount of coagulants that are formed in situ from aluminum and iron electrodes. The faster the operation for removing ions, the lower the amount of iron and aluminum that will be added to the media.

This speed at which the removal of ions occurred was mainly due to the presence of clay in the solution. As discussed earlier, the clay minerals showed fairly rapid adsorption kinetics, compared with metal ions. Thus, there is an advantage to having removal processes using hybrid systems with very short times.

3.3.1. Effect of Initial Concentration of Metal Ions. The results of the effect of the initial concentration obtained from systems using only electroflotation-coagulation with aluminum and iron electrodes and hybrid adsorption electroflotation-coagulation systems are shown in the graphs of Figures 13 and 14.

From an analysis of the graphs, it can be seen that all systems showed a similar behavior when the initial concentration of metal ions was increased. It is possible to observe

Table 5: Parameters of diffusion mechanisms from Webber-Morri model and Boyd model in adsorption of Cu(II), Ni(II), Cd(II), and Pb(II) onto sodium clay (SC) and ferric clay (FC). Experimental conditions: acetate buffer pH = 5.5, T = 28°C. Initial concentration of ions = 100 mg L^{-1}.

	Metal	Cu		Ni		Cd		Pb	
	Clay	SC	FC	SC	FC	SC	FC	SC	FC
Webber-Morri	K_1 ($mg.g^{-1}.min^{-1}$)	1.150	1.412	2.648	1.782	2.291	0.101	4.100	4.695
	C_1 ($mg.g^{-1}$)	25.73	17.53	12.28	10.50	8.676	17.98	18.774	19.83
	D_1 ($cm^2.min^{-1}$)	0.028	0.025	0.081	0.025	0.039	$9.8x10^{-5}$	0.52	0.65
	R_1^2	0.842	0.739	0.932	0.736	0.843	0.853	0.931	0.895
	K_2 ($mg.g^{-1}.min^{-1}$)	0.213	0.019	0.206	0.388	0.335	—	0.661	0.218
	C_2 ($mg.g^{-1}$)	26.79	21.23	19.24	14.33	13.9	—	28.68	21.02
	D2 ($cm^2.min^{-1}$)	$9.8 \times 10 - 6$	$4.5 \times 10 - 6$	$4.9 \times 10 - 4$	$1.2 \times 10 - 3$	$8.4 \times 10 - 4$	—	$1.3 \times 10 - 2$	$1.4 \times 10 - 3$
	R_2^2	0.764	0.978	0.967	0.926	0.974	—	0.789	0.822
Boyd	B1	0.360	0.374	0.242	0.107	0.143	0.033	0.042	0.169
	D1 ($cm^{-2}\,min^{-1}$)	$2.8 \times 10 - 6$	$2.9 \times 10 - 6$	$1.9 \times 10 - 6$	$8.5 \times 10 - 7$	$1.1 \times 10 - 6$	$2.6 \times 10 - 7$	$3.3 \times 10 - 7$	$1.3 \times 10 - 6$
	R_1^2	0.974	0.974	0.988	0.884	0.911	0.934	0.986	0.987
	B2	0.018	0.023	0.051	0.024	0.031	—	0.026	0.005
	D2 ($cm^{-2}\,min^{-1}$)	$1.4 \times 10 - 7$	$1.8 \times 10 - 7$	$4.0 \times 10 - 7$	$1.9 \times 10 - 7$	$2.5 \times 10 - 7$	—	$2.1 \times 10 - 7$	$4.5 \times 10 - 8$
	R_2^2	0.758	0.976	0.924	0.932	0.958	—	0.583	0.629

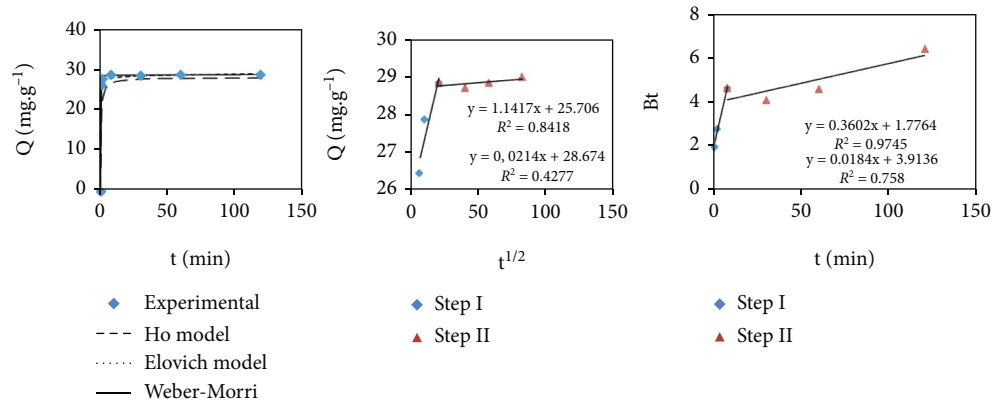

Figure 5: Experimental curves and the Ho, Elovich, and Webber-Morri models of the kinetic study of Cu(II) ion adsorption in sodium clay.

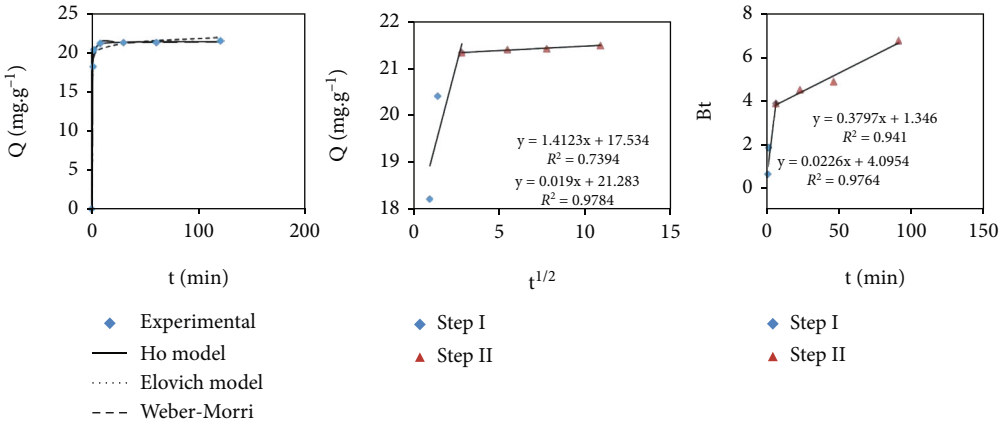

Figure 6: Experimental curves and the models of Ho, Elovich, and Webber-Morri models of the kinetic study of adsorption of the Cu(II) ion in ferric clay.

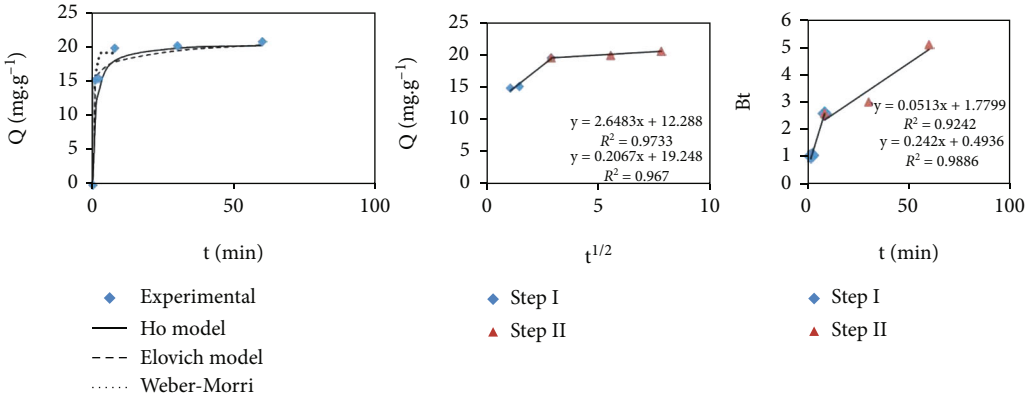

Figure 7: Experimental curves and the Ho, Elovich, and Webber-Morri models of the kinetic study of Ni(II) ion adsorption on sodic clay.

that the removal capabilities diminish when working with higher concentrations. This result is consistent, since the removal percentages are calculated from the remaining concentrations of metal ions in the solution by initial concentrations. All clays have a maximum capacity of saturation of their adsorption sites. At higher concentrations, saturation occurs after the adsorption capacity, and a greater number of ions remain in the solution than remain when working at lower concentrations. The percentage of ions that are removed is calculated from the amount that was not retained (Cf) of the initial amount (C), and at higher concentrations, these values decrease because the values (Ci) greatly increase, whereas the values of (Cf) do not decrease proportionately.

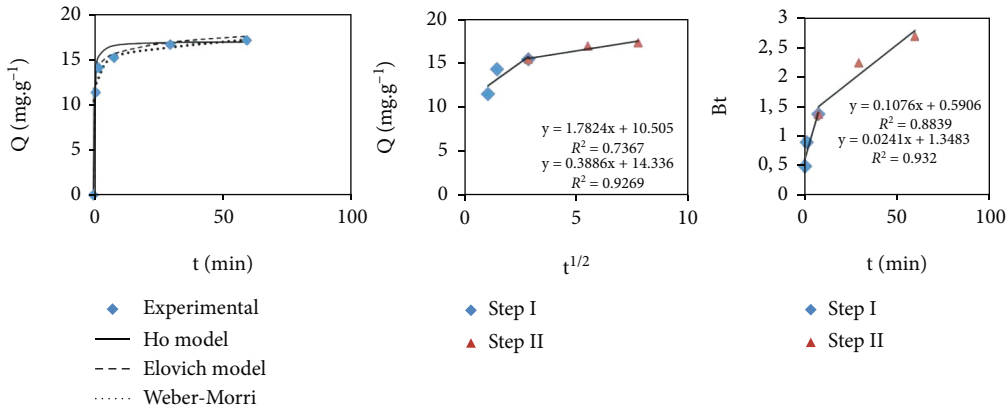

Figure 8: Experimental curves and the Ho, Elovich and Webber-Morri models of the kinetic study of Ni(II) ion adsorption in ferric clay.

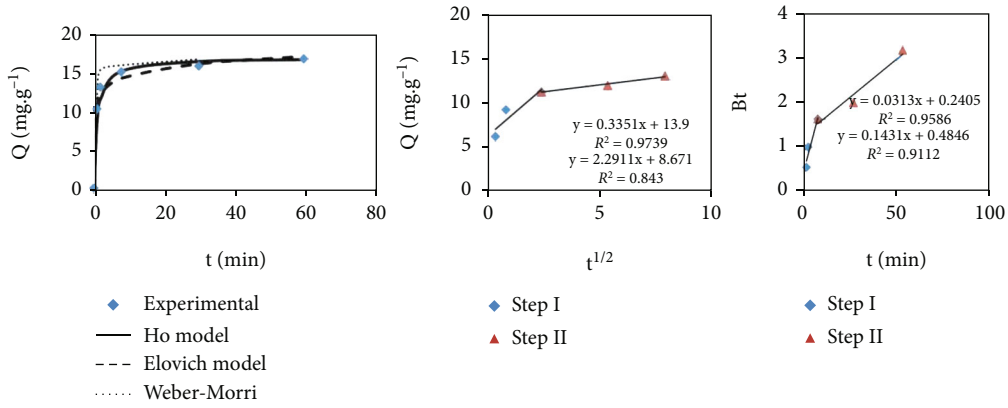

Figure 9: Experimental curves and the Ho, Elovich, and Webber-Morri models of the kinetic study of the adsorption of the Cd(II) ion in sodic clay.

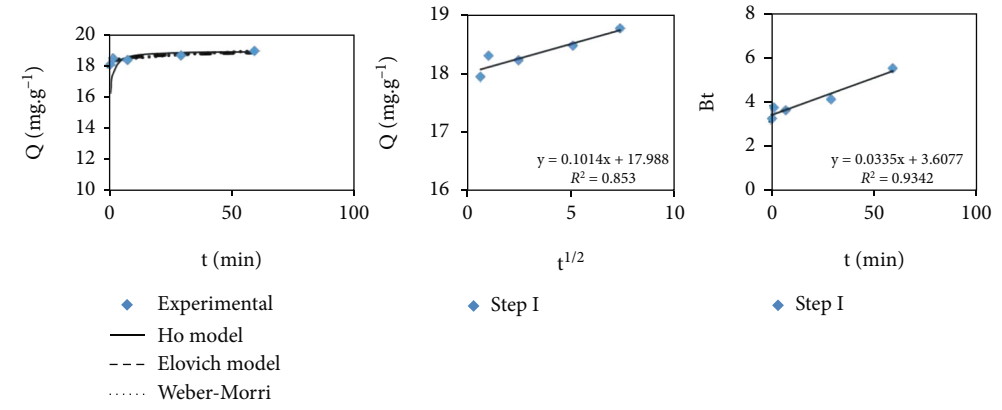

Figure 10: Experimental curves and the Ho, Elovich, and Webber-Morri models of the kinetic study of the adsorption of the Cd(II) ion in ferric clay.

In all cases, the hybrid systems promote greater removal capacity when compared to systems which use only electrodes. When using only the electrodes, the processes involved in the removal of metal ions occur from the formation of coagulants in situ agents, predominantly the electrocoagulation process [49]. Increased removal capability is noticeable when aluminum and carbon electrodes steel are utilized and then when compared to stainless steel electrode. However, when the same procedure is done with the addition of clay to the solution, there are two phenomena that

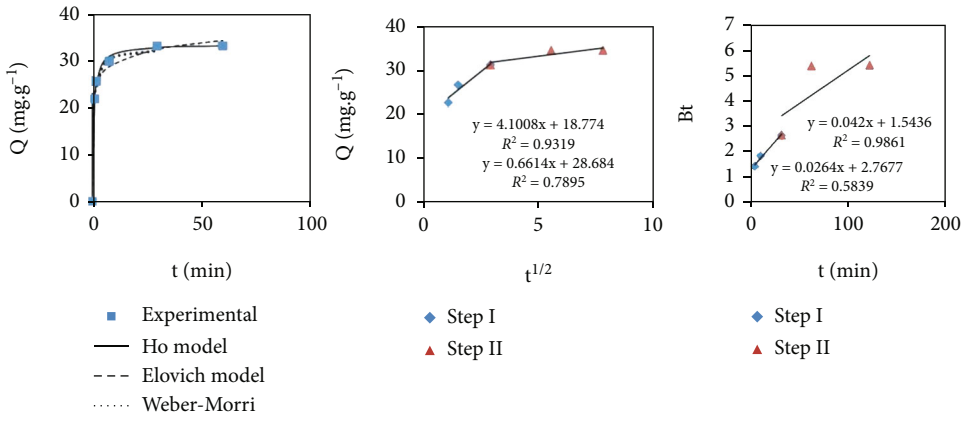

Figure 11: Experimental curves and the Ho, Elovich, and Webber-Morri models of the kinetic study of Pb(II) ion adsorption in sodic clay.

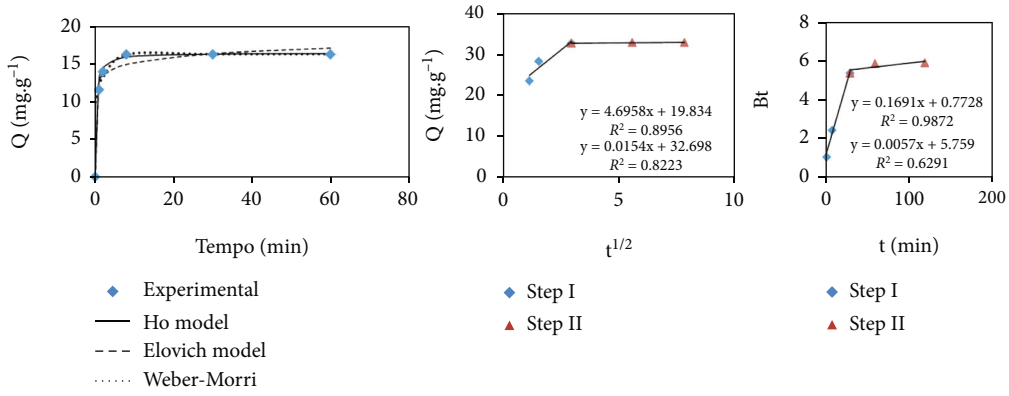

Figure 12: Experimental curves and the Ho, Elovich, and Webber-Morri models of the kinetic study of Pb(II) ion adsorption in ferric clay.

Table 6: Numerical results of tests to assess removal percentages of Cu(II), Ni(II), Cd(II), and Pb(II) from combinations clay x electrode.

	Clay	Removal percentage			
		Cu	Ni	Cd	Pb
Aluminum electrode	SC	46.88 ± 3.2	32.95 ± 2.9	16.14 ± 1.2	32.54 ± 1.5
	FC	50.11 ± 3.4	36.71 ± 2.6	21.59 ± 2.2	23.43 ± 1.3
Iron electrode	SC	32.32 ± 1.4	31.61 ± 1.0	10.32 ± 1.6	29.82 ± 1.3
	FC	33.43 ± 2.3	30.43 ± 1.6	15.94 ± 2.2	29.82 ± 1.1
Stainless steel electrode	SC	16.50 ± 0.4	17.56 ± 1.2	11.06 ± 1.1	26.78 ± 1.5
	FC	20.81 ± 0.4	15.26 ± 1.7	10.23 ± 1.3	23.43 ± 2.4

help the separation of ions from solution. There are phenomena of electroflotation-coagulation of metal ions and simultaneously the adsorption of ions in the structure of clay minerals.

Other studies have obtained similar results when used only electroflotation-coagulation processes in the removal of other ions. Aji et al. [50] studied the removal of Cu(II), Mn(II), Zn(II), and Ni(II) using an iron electrode and showed a decrease in ability removal of these ions such as increased concentration. Adhoum and Monser [51] evaluated the use of electrocoagulation for the removal of Cu(II), Zn(II), and Cr(II) using aluminum electrode and observed that higher initial concentrations of metal ions in solution will be residual remaining in the solution after a certain time of operation. Golder et al. [52] removed the ion Cr(III) by electrocoagulation with a stainless-steel electrode and showed that the percentage removal of this ion falls from 60.0 to 47.2% when the concentrations of Cr(III) is increased

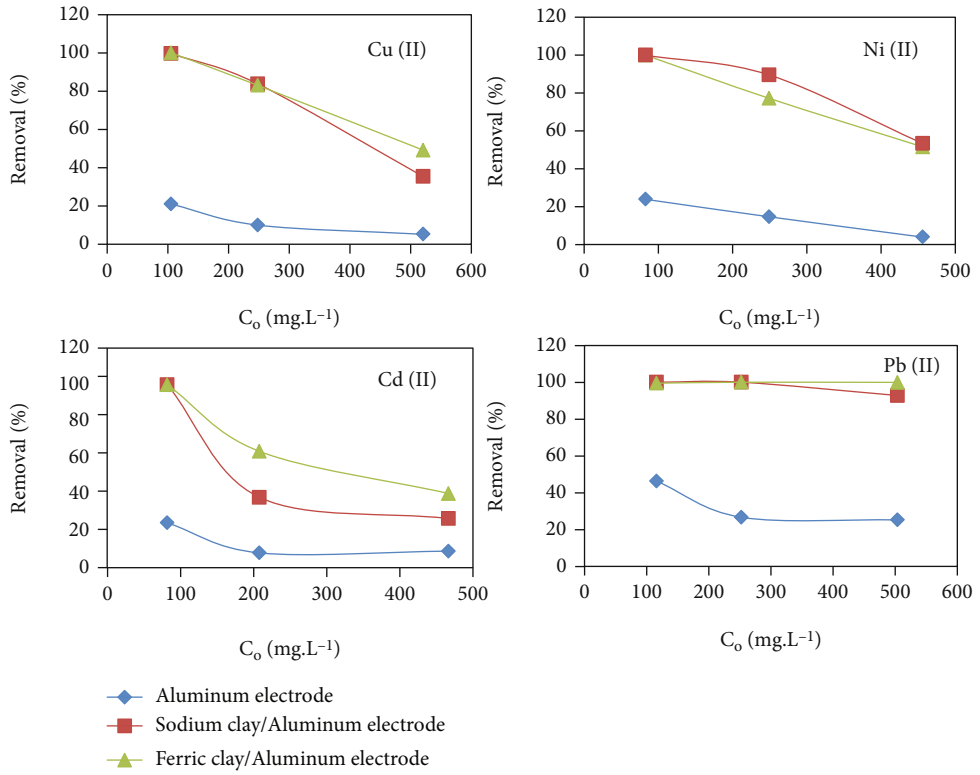

Figure 13: Percentage of removal of Cu(II), Ni(II), Cd(II), and Pb(II) ions in different systems using aluminum electrode. pH = 5.5, T = 28°C.

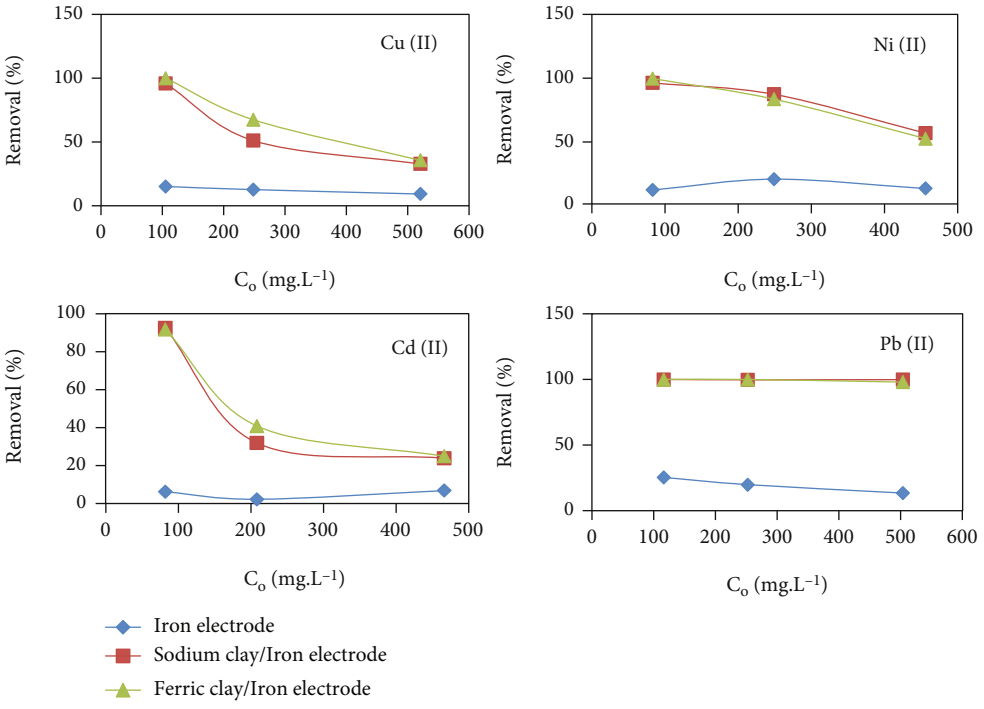

Figure 14: Percentage of removal of Cu(II), Ni(II), Cd(II), and Pb(II) ions in different systems using Iron electrode. pH = 5.5 , T = 28°C.

from 1700 to 3000 mg L^{-1}. Merzouk et al. [53] studied the removal of Cd(II), Fe(II), Ni(II), and Zn(II) using aluminum electrode and also showed a decrease in the removal capacity with increasing the initial concentrations of ions in solution.

4. Conclusion

The clays showed the fast adsorption kinetics and their good adsorption capacity. The analysis of the isotherms showed

that the experimental data were best described by the Langmuir model.

Hybrid system adsorption and electroflotation-coagulation presented itself as a good alternative association by using clay as adsorbents. This system showed that the main advantage is the possibility of working continuously with industrial wastewater purification processes, since the electrocoagulation process is more effective and produces a rapid separation of the clay from the aqueous solution. Moreover, the junction of electrocoagulation-coagulation processes to the processes of the adsorptive clays by increasing the amounts of the metal ion removal percentages.

Aluminum and iron electrodes were the ones which promoted a better removal rate when compared to stainless steel electrode. This was verified by the fact that these two types of electrodes release into the medium a greater amount of the coagulating agents than is released by the stainless steel electrode in a same time interval.

The operating times, for the removal of metal ions using the hybrid system, were very short. All maximum adsorption capacities were hit before the first ten minutes. The removal percentages varied according to the initial concentration of metal ions. The ion removal percentages for Pb(II), with iron electrode for sodium clays and ferric, were between 97 and 100%.

For the application of this technology in the industrial sector, some adjustments must be made with the operating conditions. In addition, the tailings produced after the removal of metal ions should be tested for other industrial purposes, for example, in catalysis studies and as fillers in the manufacture of materials such as ceramics.

Data Availability

The data used to support the findings of this study are available from the corresponding author upon request.

Conflicts of Interest

The authors have no conflict of interest to disclose.

Acknowledgments

This research was supported by the Basic Science Research Program through the National Research Foundation of Korea (NRF) funded by the Ministry of Education (NRF2020R1I1A2066868) and the National Research Foundation of Korea (NRF) grant funded by the Korean government (MSIT) (No. 2020R1A5A2019413). This work was financially supported by the Cearense Foundation for Support to Scientific and Technological Development e FUNCAP.

References

[1] P. C. Nagajyoti, K. D. Lee, and T. V. M. Sreekanth, "Heavy metals, occurrence and toxicity for plants: a review," *Environmental Chemistry Letters*, vol. 8, no. 3, pp. 199–216, 2010.

[2] T. A. Kurniawan, G. Y. Chan, W. H. Lo, and S. Babel, "Physico–chemical treatment techniques for wastewater laden with heavy metals," *Chemical Engineering Journal*, vol. 118, no. 1-2, pp. 83–98, 2006.

[3] H. Särkkä, B. Amit, and S. Mika, "Recent developments of electro-oxidation in water treatment—a review," *Journal of Electroanalytical Chemistry*, vol. 754, pp. 46–56, 2015.

[4] H. Chenik, M. Elhafdi, A. Dassaa, A. H. Essadki, and M. Azzi, "Removal of real textile dyes by electrocoagulation/electroflotation in a pilot external-loop airlift reactor," *Journal of Water Resource and Protection*, vol. 5, no. 10, pp. 1000–1006, 2013.

[5] V. K. Gupta, A. Nayak, and S. Agarwal, "Bioadsorbents for remediation of heavy metals: current status and their future prospects," *Environmental Engineering Research*, vol. 20, no. 1, pp. 1–018, 2015.

[6] T. A. Saleh and V. K. Gupta, "Processing methods, characteristics and adsorption behavior of tire derived carbons: a review," *Advances in Colloid and Interface Science*, vol. 211, pp. 93–101, 2014.

[7] M. Addy, B. Losey, R. Mohseni, E. Zlotnikov, and A. Vasiliev, "Adsorption of heavy metal ions on mesoporous silica-modified montmorillonite containing a grafted chelate ligand," *Applied Clay Science*, vol. 59-60, pp. 115–120, 2012.

[8] S. Lukman, M. H. Essa, N. Mu'azu, A. Bukhari, and C. Basheer, "Adsorption and desorption of heavy metals onto natural clay material: influence of initial pH," *Environmental Science & Technology*, vol. 6, no. 1, pp. 1–15, 2012.

[9] D. Ozdes, C. Duran, and H. B. Senturk, "Adsorptive removal of Cd (II) and Pb (II) ions from aqueous solutions by using Turkish illitic clay," *Journal of Environmental Management*, vol. 92, no. 12, pp. 3082–3090, 2011.

[10] E. Padilla-Ortega, R. Leyva-Ramos, and J. V. Flores-Cano, "Binary adsorption of heavy metals from aqueous solution onto natural clays," *Chemical Engineering Journal*, vol. 225, pp. 535–546, 2013.

[11] V. Hernández-Montoya, M. A. Pérez-Cruz, D. I. Mendoza-Castillo, M. R. Moreno-Virgen, and A. Bonilla-Petriciolet, "Competitive adsorption of dyes and heavy metals on zeolitic structures," *Journal of Environmental Management*, vol. 116, pp. 213–221, 2013.

[12] H. Merrikhpour and M. Jalali, "Comparative and competitive adsorption of cadmium, copper, nickel, and lead ions by Iranian natural zeolite," *Clean Technologies and Environmental Policy*, vol. 15, no. 2, pp. 303–316, 2013.

[13] D. Q. Melo, C. B. Vidal, T. C. Medeiros et al., "Biosorption of metal ions using a low cost modified adsorbent (*Mauritia Flexuosa*): experimental design and mathematical modeling," *Environmental Technology*, vol. 37, no. 17, pp. 2157–2171, 2016.

[14] A. G. Oliveira, J. Ribeiro, D. Q. Melo et al., "Evaluation of two biosorbents in the removal of metal ions in aqueous using a pilot scale fixed-bed system. Orbital: electron," *Chem*, vol. 6, pp. 47–55, 2014.

[15] T. Depci, A. R. Kul, and Y. Önal, "Competitive adsorption of lead and zinc from aqueous solution on activated carbon prepared from Van apple pulp: study in single-and multi-solute systems," *Chemical Engineering Journal*, vol. 200-202, pp. 224–236, 2012.

[16] S. F. Lo, S. Y. Wang, M. J. Tsai, and L. D. Lin, "Adsorption capacity and removal efficiency of heavy metal ions by Moso and Ma bamboo activated carbons," *Chemical Engineering Research and Design*, vol. 90, no. 9, pp. 1397–1406, 2012.

[17] M. A. Barakat, "New trends in removing heavy metals from industrial wastewater," *Chem*, vol. 4, no. 4, pp. 361–377, 2011.

[18] V. V. Keerthi and N. Balasubramanian, "Removal of heavy metals by hybrid electrocoagulation and microfiltration processes," *Environmental Technology*, vol. 34, no. 20, pp. 2897–2902, 2013.

[19] F. Han, G. H. Zhang, and P. Gu, "Removal of cesium from simulated liquid waste with countercurrent two-stage adsorption followed by microfiltration," *Journal of Hazardous Materials*, vol. 225-226, pp. 107–113, 2012.

[20] J. Charles, C. Bradu, N. Morin-Crini et al., "Pollutant removal from industrial discharge water using individual and combined effects of adsorption and ion-exchange processes: chemical abatement," *Journal of Saudi Chemical Society*, vol. 20, no. 2, pp. 185–194, 2016.

[21] P. Myllymäki, R. Lahti, H. Romar, and U. Lassi, "Removal of total organic carbon from peat solution by hybrid method—electrocoagulation combined with adsorption," *Journal of water process engineering*, vol. 24, pp. 56–62, 2018.

[22] S. Ayub, A. A. Siddique, M. S. Khursheed et al., "Removal of heavy metals (Cr, Cu, and Zn) from electroplating wastewater by electrocoagulation and adsorption processes," *Water Treat*, vol. 179, no. 1, pp. 263–271, 2020.

[23] E. M. Nigri, A. L. A. Santos, and S. D. F. Rocha, "Removal of organic compounds, calcium and strontium from petroleum industry effluent by simultaneous electrocoagulation and adsorption," *Journal of Water Process Engineering*, vol. 37, article 101442, 2020.

[24] P. Rengasamy and G. J. Churchman, *Cation exchange capacity, exchangeable cations and sodicity*, CSIRO Publishing, 1999.

[25] A. N. Oo, C. B. Iwai, and P. Saenjan, "Soil properties and maize growth in saline and nonsaline soils using cassava-industrial waste compost and vermicompost with or without earthworms," *Land Degradation and Development*, vol. 26, no. 3, pp. 300–310, 2015.

[26] V. B. Bagdonavicius and M. S. Nikulin, "Chi-squared goodness-of-fit test for right censored data," *The International Journal of Applied Mathematics and Statistics*, vol. 24, 2011.

[27] R. R. Karri, J. N. Sahu, and N. S. Jayakumar, "Optimal isotherm parameters for phenol adsorption from aqueous solutions onto coconut shell based activated carbon: error analysis of linear and non-linear methods," *Journal of the Taiwan Institute of Chemical Engineers*, vol. 80, pp. 472–487, 2017.

[28] L. Alexandrova and L. Grigorov, "Precipitate and adsorbing colloid flotation of dissolved copper, lead and zinc ions," *International Journal of Mineral Processing.*, vol. 48, no. 1-2, pp. 111–125, 1996.

[29] O. Sahu, B. Mazumdar, and P. K. Chaudhari, "Treatment of wastewater by electrocoagulation: a review," *Environmental Science and Pollution Research*, vol. 21, no. 4, pp. 2397–2413, 2014.

[30] G. W. Brindley and M. Nakahira, "The kaolinite-mullite reaction series: I, a survey of outstanding problems," *Journal of the American Ceramic Society*, vol. 42, no. 7, pp. 311–314, 1959.

[31] G. A. Lager, J. D. Jorgensen, and F. J. Rotella, "Crystal structure and thermal expansion of α-quartz SiO_2 at low temperatures," *Journal of Applied Physics*, vol. 53, no. 10, pp. 6751–6756, 1982.

[32] J. D. Hanawalt, H. W. Rinn, and L. K. Frevel, "Chemical analysis by X-Ray diffraction," *Industrial & Engineering Chemistry Analytical Edition*, vol. 10, no. 9, pp. 457–512, 1938.

[33] E. Teixeira-Neto and A. A. Teixeira-Neto, "Modificação química de argilas: desafios científicos e tecnológicos para obtenção de novos produtos com maior valor agregado," *Química Nova*, vol. 32, no. 3, pp. 809–817, 2009.

[34] H. E. Swanson, E. Tatge, and R. K. Fuyat, *Standard x-ray diffraction powder patterns*, U.S. Department of commerce, 1953.

[35] S. K. Sing, D. H. Everett, R. Haul et al., "Reporting physisorption data for gas/solid system," *Pure and Applied Chemistry*, vol. 57, pp. 603–619, 2008.

[36] J. Langmuir, "The adsorption of gases on planes of glassmica and platinium," *Journal of the American Chemical Society*, vol. 40, no. 9, pp. 1361–1403, 1918.

[37] H. M. F. Freundlich, "Über die adsorption in Lösungen," *The Journal of Physical Chemistry*, vol. 57U, no. 1, pp. 385–470, 1907.

[38] M. J. Temkin and V. Pyzhev, "Recent modifications to Langmuir isotherms," *Acta physicochimica*, vol. 12, pp. 217–222, 1940.

[39] H. E. Rybicka, W. Calman, and A. Breeger, "Heavy metals sorption/desorption on competing clay minerals; an experimental study," *Applied Clay Science*, vol. 9, no. 5, pp. 369–381, 1995.

[40] J. H. Potgieter, S. S. Potgieter-Vermaak, and P. D. Kalibantonga, "Heavy metals removal from solution by palygorskite clay," *Minerals Engineering*, vol. 19, no. 5, pp. 463–470, 2006.

[41] Y. S. E. Ho and G. Mckay, "Sorption of dye from aqueous solution by peat," *Chemical Engineering Journal*, vol. 70, no. 2, pp. 115–124, 1998.

[42] S. Z. Roginsky and J. Zeldovich, "An equation for the kinetics of activated adsorption," *Acta Physicochimica*, vol. 1554, pp. 554–559, 1934.

[43] D. Q. Melo, C. B. Vidal, A. L. Silva et al., "Removal do Cd^{+2}, Cu^{+2}, Ni^{+2} and Pb^{+2} ions from aqueous solutions using Tururi fibers as an adsorbent," *Journal of Applied Polymer Science*, vol. 131, no. 20, 2014.

[44] H. Chen and A. Wang, "Kinetic and isothermal studies of lead ion adsorption onto palygorskite clay," *Journal of Colloid and Interface Science*, vol. 307, no. 2, pp. 309–316, 2007.

[45] W. J. Weber Jr. and J. C. Morris, "Kinetics of adsorption on carbon from solution," *Proceedings of the American Society of Civil Engineers*, vol. 89, no. 2, pp. 31–59, 1963.

[46] G. E. Boyd, J. Schubert, and A. W. Adamson, "The exchange adsorption of ions from aqueous solutions by organic zeolites, I: Ion exchange equilibria," *Journal of the American Chemical Society*, vol. 69, no. 11, pp. 2818–2829, 1947.

[47] F. Salles, J. M. Douillard, O. Bildstein et al., "Diffusion of interlayer cations in swelling clays as a function of water content: case of montmorillonites saturated with alkali cations," *The Journal of Physical Chemistry*, vol. 119, no. 19, pp. 10370–10378, 2015.

[48] E. D. Glendening and D. Feller, "Cation-water interactions: the $M^+(H_2O)_n$ clusters for alkali metals, M= Li, Na, K, Rb, and Cs," *The Journal of Physical Chemistry*, vol. 99, no. 10, pp. 3060–3067, 1995.

[49] M. Mollah and A. Yousuf, "Electrocoagulation (EC)- science and applications," *Journal of Hazardous Materials*, vol. 84, no. 1, pp. 29–41, 2001.

[50] A. B. Aji, Y. Yavuz, and A. S. Koparal, "Electrocoagulation of heavy metals containing model wastewater using monopolar iron electrodes," *Separation and Purification Technology*, vol. 86, pp. 248–254, 2012.

[51] N. Adhoum and L. Monser, "Decolourization and removal of phenolic compounds from olive mill wastewater by electrocoagulation," *Chemical Engineering and Processing*, vol. 43, no. 10, pp. 1281–1287, 2004.

[52] A. K. Golder, A. N. Samanta, and S. Ray, "Removal of trivalent chromium by electrocoagulation," *Separation and Purification Technology*, vol. 53, no. 1, pp. 33–41, 2007.

[53] B. Merzouk, B. Gourich, A. Sekki, K. Madani, and M. Chibane, "Removal turbidity and separation of heavy metals using electrocoagulation–electroflotation technique: a case study," *Journal of Hazardous Materials*, vol. 164, no. 1, pp. 215–222, 2009.